Miniaturized Photonic and Microwave Integrated Circuits Based on Surface Plasmon Polaritons

**Da Yue Yao[1, 2], Pei Hang He[1, 2], Hao Chi Zhang[1, 2, *],
Jia Wen Zhu[1, 2], Mingzhe Hu[3, *], and Tie Jun Cui[1, 2, *]**

Abstract—Photonic integrated circuits (PICs) and microwave integrated circuits (MICs) have been widely studied, but both of them face the challenge of miniaturization. On one hand, the construction of photonic elements requires spaces proportional to wavelength, and on the other hand, electromagnetic compatibility issues make it challenging to reach high-density layouts for MICs. In this paper, we review the research advances of miniaturized PICs and MICs based on surface plasmon polaritons (SPPs). By introducing SPPs, miniaturized photonic elements at subwavelength scales are realized on PICs, which can be used for highly integrated interconnects, biosensors, and visible light wireless communications. For MICs, since the metals behave as perfect conductors rather than plasmonic materials at microwave frequencies, plasmonic metamaterials are proposed to support spoof SPPs. Spoof SPPs possess similar characteristics to SPPs and can be used to realize high-density channels on MICs. Moreover, combining the latest theoretical research on SPPs, future tendencies of SPP-based MICs are discussed as well, including further miniaturization, digitization, and systematization.

1. INTRODUCTION

With rapid developments of modern wireless communications [1], optical computing [2] and biosensing [3], photonic (waves with frequencies between 300 GHz and 750 THz) integrated circuits (PICs) [4–7], and microwave(waves with frequencies between 300 MHz and 300 GHz) integrated circuits (MICs) [8–10] have been widely studied. On one hand, PICs with photons as information carriers have become the limelight due to their advantages such as high response rates, fast transmission speeds, high parallelism, and excellent compatibility [11–15]. Data moves in a photonic device at the speed of light, about ten times faster than electrons in a standard circuit [16]. Ref. [17] has demonstrated a universal optical vector convolutional accelerator operating at more than ten TOPS (trillions (10^{12}) of operations per second, or tera-ops per second). Ref. [18] has demonstrated mode-division multiplexing circuits based on digitized meta-structures with extremely compact footprints. It can reduce the size of critical components by 1–2 orders of magnitude and realize dense wiring of 3×112 Gbit/s high-speed mode division multiplexing signal, which is conducive to large-scale on-chip integration of multimode optical systems. However, the construction of photonic elements requires spaces proportional to wavelength. To propagate the wavelength of communication band, the size of optical devices must be on the order of microns, which is difficult to integrate on optoelectronic integrated chips. Thus, the conventional photonics devices are constrained by the classical diffraction limit, resulting in large sizes of PICs. On the other hand, MICs have the advantage of easy connection to wireless devices [19–21]. But with the

explosive increase of information data in modern communication systems, the development of MICs faces the challenges such as spatial coupling, dynamic response, and performance robustness, among which the contradiction between miniaturization of MICs and electromagnetic compatibility is particularly prominent [22–24]. The contradiction caused by the physical characteristics of high-frequency elements has become one of the main obstacles to the development of MICs.

The introduction of surface plasmon polaritons (SPPs) [25–30] is expected to contribute to the miniaturized PICs and MICs. SPPs are surface waves produced by the collective resonance of electrons and electromagnetic waves on the interfaces of metals and dielectrics, which can strongly confine the electromagnetic energy in the subwavelength range of the interface. The novel field of plasmonics has recently emerged, in consideration of the progress of new materials, including topological Dirac semimetals [31–36], two-dimensional (2D) materials [37–41], topological insulators [42, 43], and Dirac materials [44–47]. Ref. [44] has predicted a novel undamped gapless plasmon mode in a type-II Dirac semimetal, arising from the presence of both electron and hole pockets at the Fermi energy. Ref. [48] has discovered that the plasmon frequency can be tuned when chemical species are adsorbed at NbAs and TaAs surfaces, highlighting the high potential of topological Weyl semimetals plasmonic modes in the field of sensors. SPPs have the characteristics of field enhancement, field confinement, and slow-wave properties, which can be utilized to overcome the PIC miniaturization problem. Since the wavelength of SPPs is shorter than the wavelength of free beam in vacuum, it can overcome diffraction limit of traditional optics and is expected to realize miniaturized PICs [49, 26]. In microwave band, the properties of metals are close to perfect conductors, which makes metals incapable of exciting SPPs. This problem was not solved until 2004 when the concept of spoof SPPs was proposed by Pendry et al. [50]. By introducing plasmonic metamaterials, the properties of SPPs can be imitated at microwave frequencies, and adjusting the size of plasmonic metamaterials allows the manipulation of electromagnetic waves [51–58]. In terms of mode characteristics, the inherent field confinement of spoof SPPs has potential to resolve the contradiction between microwave devices' miniaturization and electromagnetic compatibility. In 2013, Shen et al. further proposed an ultrathin spoof SPP transmission line that can transmit spoof SPPs on planar or curved surfaces [59, 60], which makes it possible to apply spoof SPPs on planar circuits and MICs.

In this paper, we review the miniaturized PICs and MICs based on SPPs and spoof SPPs, respectively. For PICs, SPPs enable the generation, transmission, modulation, and detection of light at subwavelength scales, which can be applied to highly integrated interconnects, biosensing fields, and even visible light wireless communication systems. For MICs, the research of spoof SPPs is focused on transmission lines, the devices, and I/O interconnects. Moreover, the future tendency of SPP-based PICs and MICs is discussed as well.

2. PICS BASED ON SPP MODES

SPPs are capable of generating, distributing, modulating, and detecting light on the subwavelength scale [61, 62]. As a result, SPP technology has made a significant impact on developing miniaturized PICs [63]. A number of new structures based on SPPs have been proposed, including metallic slot waveguides [64–66], channel SPP waveguides [67], and wedge SPP waveguides [68]. Although these waveguides can provide tight optical confinement, they suffer from considerable propagation losses, which poses a challenge to further device integration. A three-dimensional SPP waveguide structure was proposed in [69], whose propagation length (defined as the propagation distance through which the amplitude of the field attenuates to $1/e$; a smaller propagation length means a considerable loss of the guided mode) is only 6 μm. Hybrid plasmonic waveguides have been proposed to enable subwavelength modes with relatively low loss [70–72], which could play a significant role in realizing deep subwavelength scale optical interconnects. The hybrid plasmonic waveguides are designed using plasmonic waveguide structures and high refractive index dielectric nanostructures [73]. The characteristics of the hybrid mode can be changed from dielectric-like to SPP-like by adjusting the mix between SPP and waveguide modes [74]. Their structures are smaller than some dielectric nanophotonic devices for the same properties such as field enhancement and low crosstalk. Plasmonic nanolasers [75, 76] based on such structures and various functional passive devices such as directional couplers [77, 78], Y-switches [79], and ring resonators [77], have been intensively investigated, as shown in Fig. 1. In [73], a novel hybrid
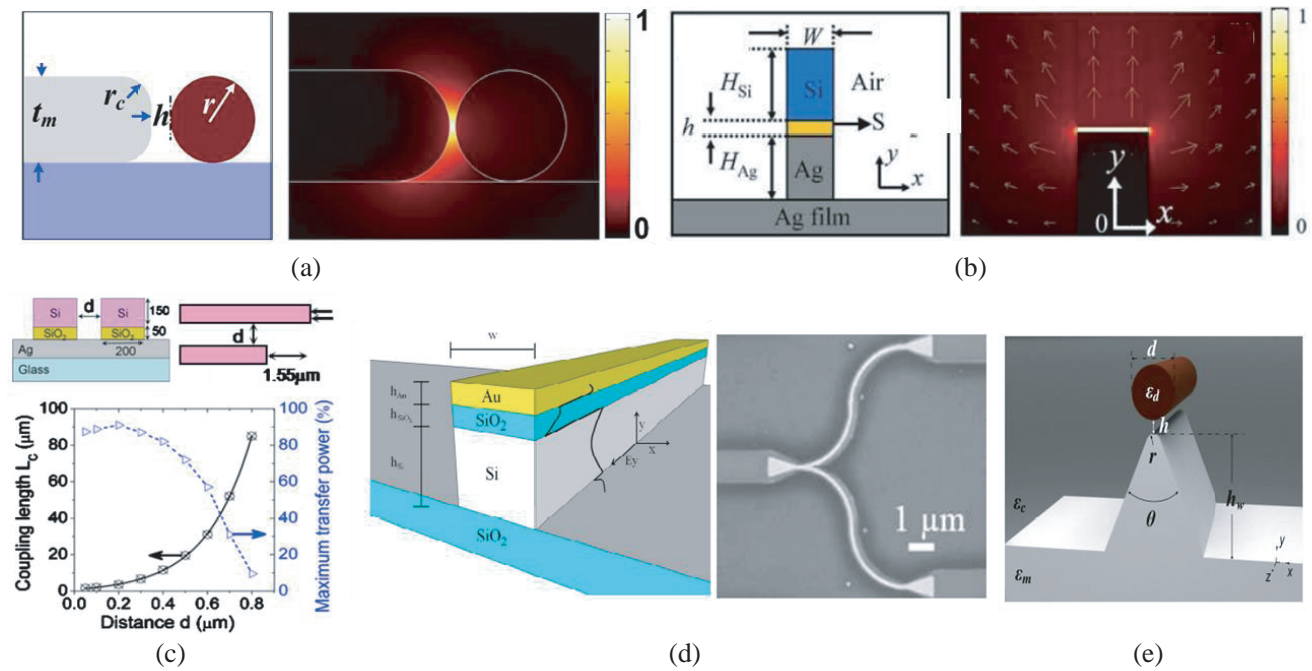
Figure 1. The structure of SPP waveguides. (a) Geometry of the proposed nanolaser [76]. (b) Schematic diagram of the waveguide [77]. (c) Schematics of the directional coupler and dependence of the coupling length L and maximum transmitted power on the separation distanced [78]. (d) Conductor-gap-silicon plasmonic waveguide structure showing the E_y field distribution of the quasi-TM mode and image of a fabricated Y-splitter with 2 μm bending radius [79]. (e) Geometry of the proposed hybrid waveguide [73].

plasmonic waveguide consisting of high refractive index nanowires placed on a triangular metallic wedge substrate has been proposed, and its propagation constant can reach 40 μm. The strong coupling between wedge-shaped plasmonic excitations and dielectric nanowire modes leads to ultra-tight confinement and low transmission loss.

The metal-based plasmonic waveguides that can be used as transmission lines for optical and electrical signals exhibit low-crosstalk transmissions and can be fabricated with complementary metal oxide semiconductor (CMOS) techniques [80]. Ref. [81] has investigated a plasmonic demultiplexer structure based on Metal-Insulator-Metal waveguides and circular ring resonators, and the mean value of crosstalk is estimated −26.95 dB. In Fig. 2, a variety of plasmonic devices are introduced, including emitters [82, 83], detectors [84, 85], and modulators [86, 87]. Plasmonic devices can integrate with photonic silicon substrates [88] by using modern micro-nano processing technology and chip manufacturing process. They have the advantages of being ultra-compact and cost saving, but the disadvantage is that they are not conducive to the manufacture of 3D structures. Ref. [84] has demonstrated an entirely new method to achieve bright visible light emission in 'bulk-sized' silicon coupled with plasmon nanocavities at room temperature, from non-thermalized carrier recombination. Ref. [86] has demonstrated a compact high-speed phase modulator, and its modulation frequency response is flat up to 65 GHz and beyond. A silicon nanoplasmonic electrooptic modulator has been designed in [87]. Ref. [89] has presented a gold/silicon based monolithic integrated circuit consisting of a gold film plasmonic waveguide. It is demonstrated that SPPs can be used as a coherent carrier in a circuit, capable of providing highly integrated optical interconnects for data processing applications.

The metal structures based on surface plasmon excitations have attracted significant attention due to their apparent advantages in high-density optical integration and can constitute a powerful detection and analysis tool in the form of optical sensors [90–93]. Sensors using SPP metal structures have enormous field enhancement benefits. But the conventional SPP sensors must work at the resonant wavelengths to maintain high sensitivities, thus they have fixed or narrow bandwidth, which limits their
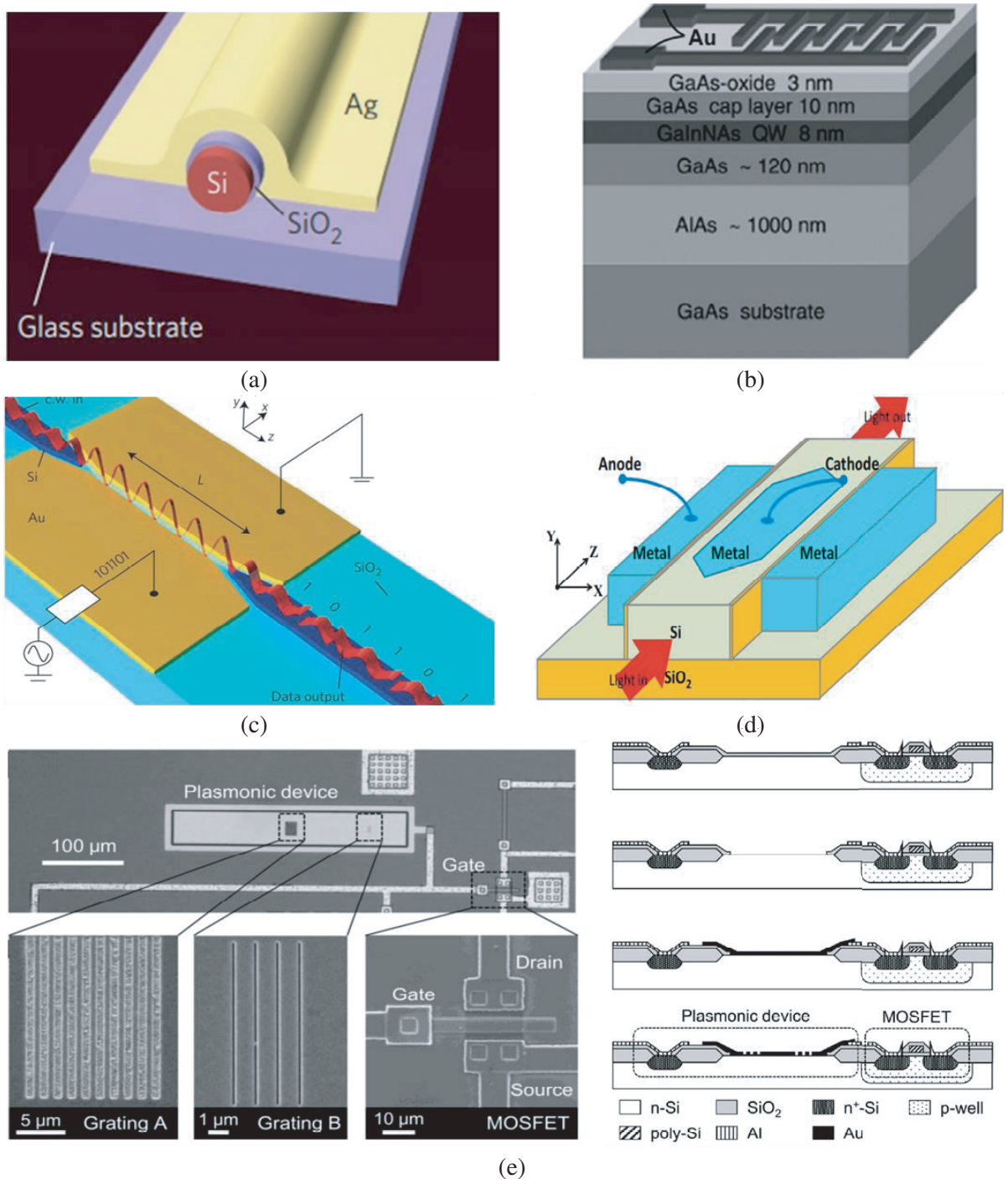
Figure 2. On-chip SPP devices. (a) Schematic of a plasmonic nanocavity-coupled silicon nanowire device [83]. (b) Metal-semiconductor-metal SPP detector [84]. (c) Schematic of the plasmonic phase modulator [86]. (d) Three-dimensional schematic of the proposed Si nanoplasmonic modulator [87]. (e) Integrated device fabrication process flow [89].

spectral capabilities and practical applications in sensing greatly. For instance, Ref. [94] has reported the plasmonic detection of single molecules in real time. Photothermal microscopy relies on the change in intensity of a detection beam (693 nm) caused by a time-dependent thermal lens. This thermal lens is created by a modulated heating beam (785 nm) that is absorbed by the nanorod. This problem can
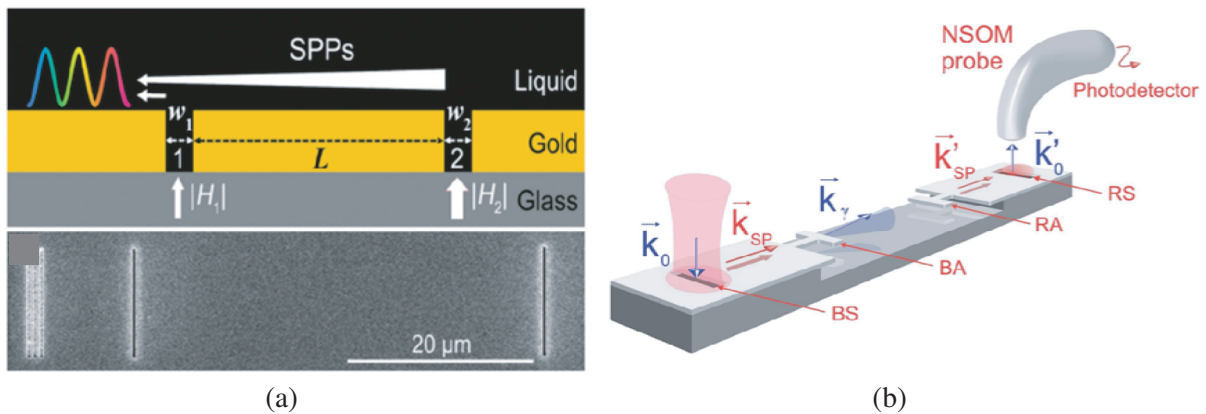
Figure 3. On-chip SPP sensing and communication components. (a) Schematic and geometric parameters of the double-slit structure on a metal film [96]. (b) Schematic representation of the nanoscale wireless communication system [99].

be solved by using array structures at the expense of large volumes (double-hole array with a 800 nm periodicity [95]), which make them difficult to be applied in integrated circuits. Fig. 3 exhibits several methods to overcome the problem of narrow band and large volume. SPP interferometry has been considered as a feasible method to overcome this massive structure. In [96], a high-contrast and broadband on-chip sensor based on the SPP interference in a metallic double-slit structure has been presented. The propagation loss of SPPs is compensated by adjusting the position of the spot of p-polarized light on the double-slit structure, and the interfering SPPs from both slits have almost equal intensity. This high contrast, broadband, and high sensitivity plasmon sensor fabricated on a subwavelength plasmonic waveguide can be easily integrated with chips. Visible light can be used for system miniaturization as well. The utilization of SPPs could enable modern on-chip wireless communication systems at visible wavelengths, reducing losses and promising miniaturization of communication systems [97, 98]. A nanoscale wireless communication system that operates at visible wavelengths via in-plane information transmission (at bandwidths in the Hz and MHz ranges) has been reported [99].

To meet the challenges of parallelism and high data rates, next-generation optical communication networks will require the joint integration of electronics and photonics, as shown in Fig. 4. When electronics and photonics are integrated, heterogeneous integration is usually used. Unfortunately, the direct modulation sources using heterogeneous integration methods are limited by bandwidth, which makes it difficult to achieve higher data rates. So far, heterogeneous transmitters in a bondwire assembly have shown the highest symbol rates of 222 GBd with plasmonics [100]. However, parasitic growth at the interface of mismatched bonding lines ultimately constitutes a speed bottleneck. Monolithic integration can overcome this bottleneck and achieve higher symbol rates using ultra-short direct connections (called on-chip vias). CMOS technology enables the efficient monolithic integration of electrons and photons. In particular, a full photonic library running on a CMOS platform with a 10 GBd data link [101] and 40 GB/s modulation [102] have been demonstrated. However, the limited bandwidth of standard CMOS technology does not allow for the symbol rates of high-speed heterogeneous demonstrations. Therefore, alternative monolithic solution relying on bipolar CMOS (BiCMOS) technology is of interest. BiCMOS technology may be of particular value as it offers high speed electronics and is compatible with CMOS. Meanwhile, SPP technology is an ideal counterpart to photonic technology [103] and compatibility with a variety of substrate materials. In [104], a monolithically integrated electro-optical transmitter based on SPPs is reported to achieve the combination of advanced BiCMOS with silicon plasmonic electronics through the co-design of an electronic and plasmonic electronics layer. Among them, the electronic layer provides BiCMOS circuitry designed to meet data centre standards and performs 4 : 1 power multiplexing to pass the on-off key control signal to the plasmonic layer above; the plasmonic layer consists of a compact, high bandwidth plasmonic Mach-Zendel modulator, and the electronic and plasmonic layers are interconnected by vias. Overall, the introduction of SPPs provides an effective way to break the speed limitations of current miniaturized transceiver systems.
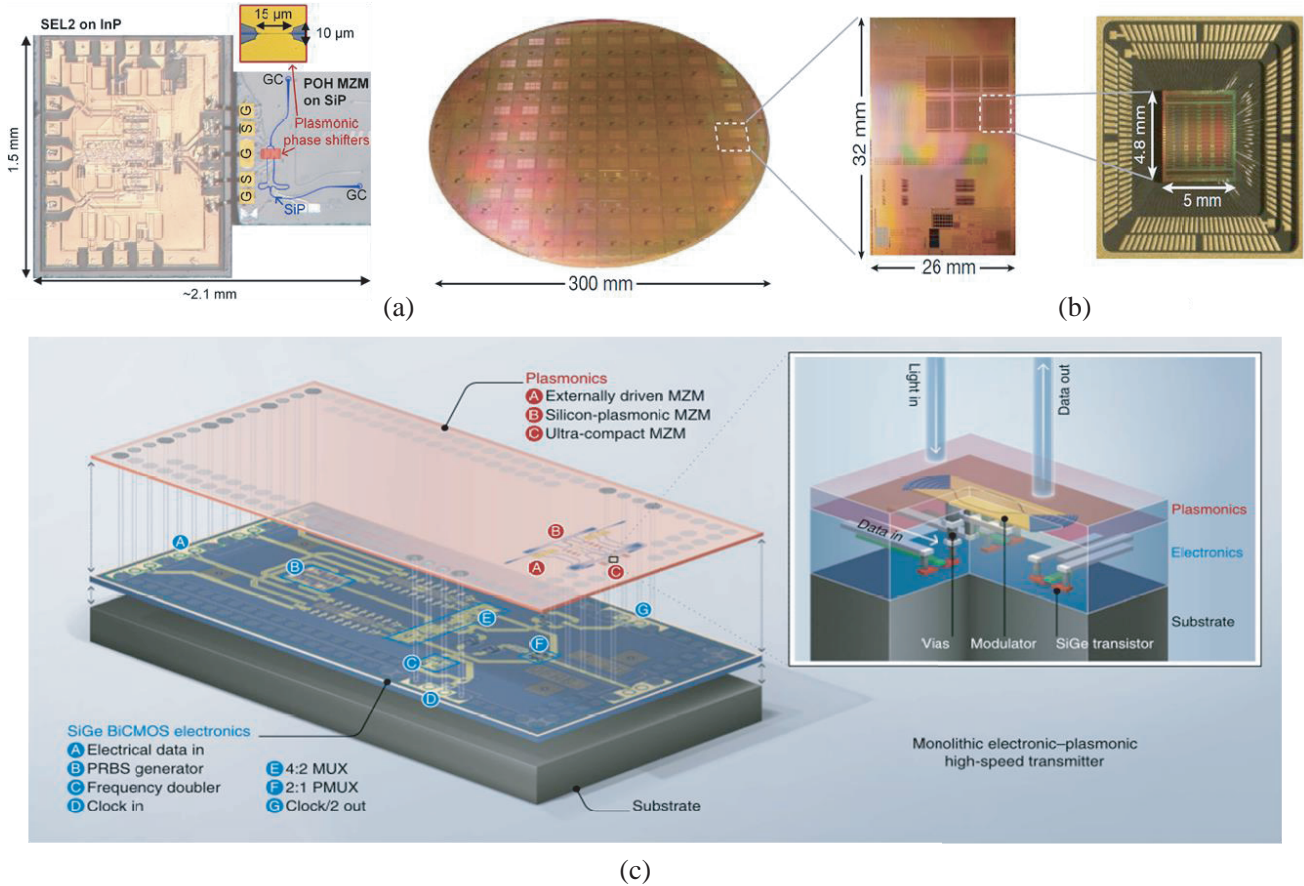
Figure 4. (a) The schematic of transmitter [100]. (b) Monolithic electronic-photonic platform in 65-nm bulk CMOS [101]. (c) Monolithic electronic-plasmonic high-speed transmitter. High-speed SiGeBiCMOS electronic layers (blue) with a top plasmonic layer (red) monolithically integrated on a common substrate (black) and connected through on-chip vias (cylinders) [104].

In summary, the miniaturized PICs based on SPPs have been widely studied. The SPP waveguides, including hybrid wedge plasmonic waveguide and gold film plasmonic waveguide, have been extensively investigated. The SPP structures can constitute highly integrated optical sensors that find important applications in environmental monitoring, biomedical and chemical research. In addition, the introduction of SPPs can miniaturize modern on-chip wireless communication systems at visible wavelengths.

3. MICS BASED ON SPOOF SPP MODES

In microwave band, both bulk spoof SPP metamaterials [105] and ultrathin spoof SPP transmission lines are utilized to transmit waves with tight confinement, as shown in Fig. 5. Considering the processing technology of ICs, ultrathin spoof SPP transmission lines are preferred on MICs.

In terms of transmission line, the most fundamental component in MICs, there is a low impedance path between metal layer and lossy substrate in the typical CMOS process, resulting in narrow band and high loss [106]. As the representatives of traditional planar microwave transmission lines, the microstrip and coplanar waveguide (CPW) have fixed space wave modes, and the transmission of electromagnetic wave is mainly distributed in the surrounding space or medium. However, in the high-density integrated circuit with a multi-layer structure that contains a large number of parallel transmission lines, the reduction of line spacing caused by miniaturization will lead to the enhancement of mutual coupling between neighbors, which will affect the overall performance of the system. Hence, the width of metal
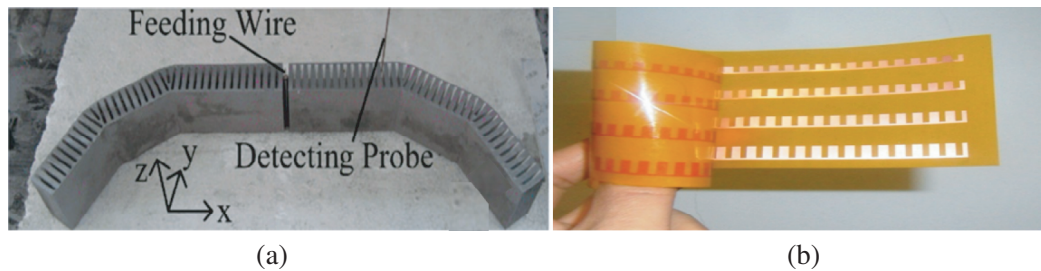
Figure 5. The spoof SPP structure of different dimensions. (a) Three dimensional spoof SPP structure [105]. (b) Flexible ultra-thin spoof SPP transmission line [59].

transmission line and the distance between the lines should not be too narrow in order to avoid ohmic loss and electromagnetic coupling caused by the skin effect at high frequencies which is contrary to the requirements of chip miniaturization. In 2015, Liang et al. firstly proposed an on-chip spoof SPP transmission line in the microwave frequency. By introducing a periodic subwavelength structure on the metal transmission line, spoof SPPs are excited and transmit signals through strong local surface waves, which can achieve a transmission line with high integration, low loss, and low crosstalk [107].

As shown in Fig. 6, two coupled spoof SPP transmission lines and two coupled quasi-TEM transmission lines are fabricated on the chip, each with a spacing of $2.4\,\mu m$, using standard $65\,nm$ CMOS technology [107]. The measured results show that the spoof SPP transmission line achieves a wideband reflection coefficient of less than $14\,dB$ and a cross checker ratio of better than $24\,dB$, ranging from $220\,GHz$ to $325\,GHz$, with an average of $19\,dB$ lower than the conventional transmission line. When multiple interconnects are placed together at high operating frequencies, cross talk can seriously distort the signal integrity. Compact and broadband spoof SPP transmission lines have the potential to replace the traditional on-chip transmission lines to meet the stringent requirements of dense interconnection at high operating frequencies for future high-performance computer servers. The compact and wideband spoof SPP transmission lines demonstrate great potentials in implementing the high-density on-chip sub-terahertz communications in CMOS.

For CMOS THz I/O links (shown in Fig. 7) which control transmitter side surface wave radiation, efficient conversion from TEM waves to surface waves is required. In the absence of mode conversion, large transmission losses can occur. The transmission of SSP coupler proposed in [108] has over $3\,dB$ loss at around $300\,GHz$ without mode conversion. However, designing a terahertz mode converter in CMOS is not easy. The high refractive index silicon substrate reduces the space field limitation of spoof SPP and makes conversion difficult. The converter design reported in [109–111] is only validated at the PCB level, requires huge ground geometry (mm order of magnitude), but is not feasible for chip level designs in CMOS. Ref. [112] reports a low loss, high integration on-chip CMOS sub-terahertz spoof SPPs converter designed and manufactured in a standard $65\,nm$ CMOS process. A novel and compact planar gradient groove with underlying grounding is developed for on-chip mode conversion in CMOS. In order to match the impedance, a mode converter structure with a smooth bridge between $50\,\Omega$ ground coplanar waveguide (GCPW) and spoof SPP transmission line is proposed. The compact wideband spoof SPP transmission lines with mode converters show great potential to replace existing transmission lines as future on-chip terahertz interconnects.

The traditional TEM-based I/O communication (via PCB traces or free space) has significant path loss and electromagnetic interference, which is challenging to be used for low-power and dense I/O interface interconnections for data servers [113]. Recently, optical [114], RF (radio frequency) [115], and baseband [116] I/O transceivers have been proposed. Although optical interconnects have shown great potential to replace electrical interconnects with high data throughput, their signal source transmission and detection are difficult to be implemented in silicon. All the blocks of RF interconnects can be implemented in CMOS operating at frequencies up to the millimeter wave region, but CMOS back-end lines are typically very thin, leading to high losses and significant electromagnetic crosstalk. In contrast, broadband high-speed interconnects with conventional transmission lines in CMOS suffer from severe electromagnetic crosstalk between narrow silicon channels compared to RF interconnects. The spoof SPP interconnect is supposed to be an up-and-coming option for future inter-chip terahertz-level data
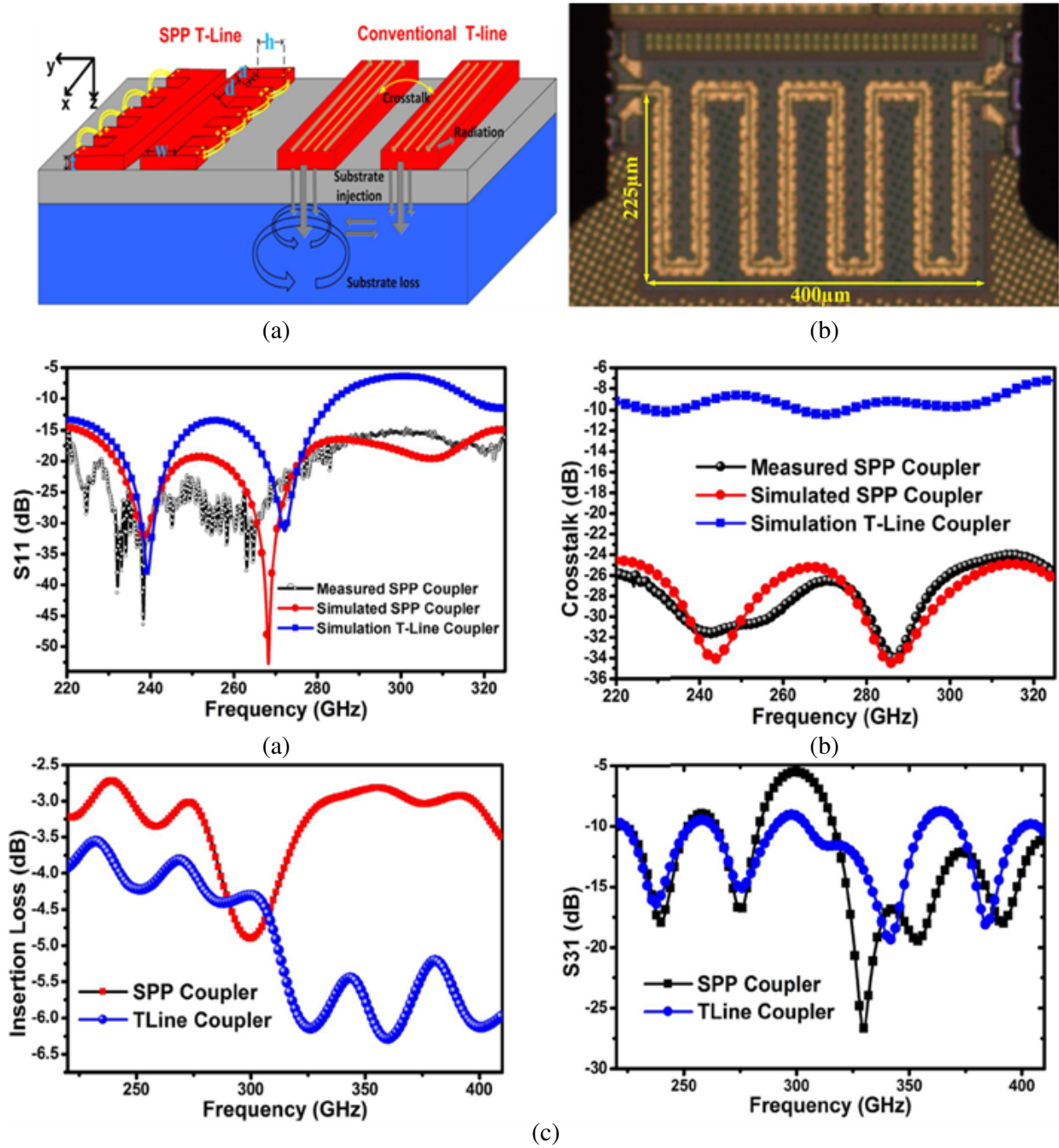
(a)

(b)

(a)

(b)

(c)

Figure 6. On-chip spoof SPP/conventional transmission line [107]. (a) The layout and E-field distribution of the on-chip spoof SPP/conventional transmission line in lossy substrate environment. (b) Die micrograph of the spoof SPP-based coupler in 65 nm CMOS for Terahertzes applications. (c) Measured and fitting S parameter results.

transmission.

A CMOS sub-terahertz spoof SPP interconnect has been proposed [113] using the spoof SPP transmission lines, mode converters, sources, and modulators. The spoof SPP transmission lines are able to confine the electromagnetic waves to periodic trenches and strongly suppress the mutual crosstalk between channels as shown in Fig. 8. It can significantly reduce the power and area. The results demonstrate the proposed CMOS sub-THz surface-wave interconnects for future data servers with
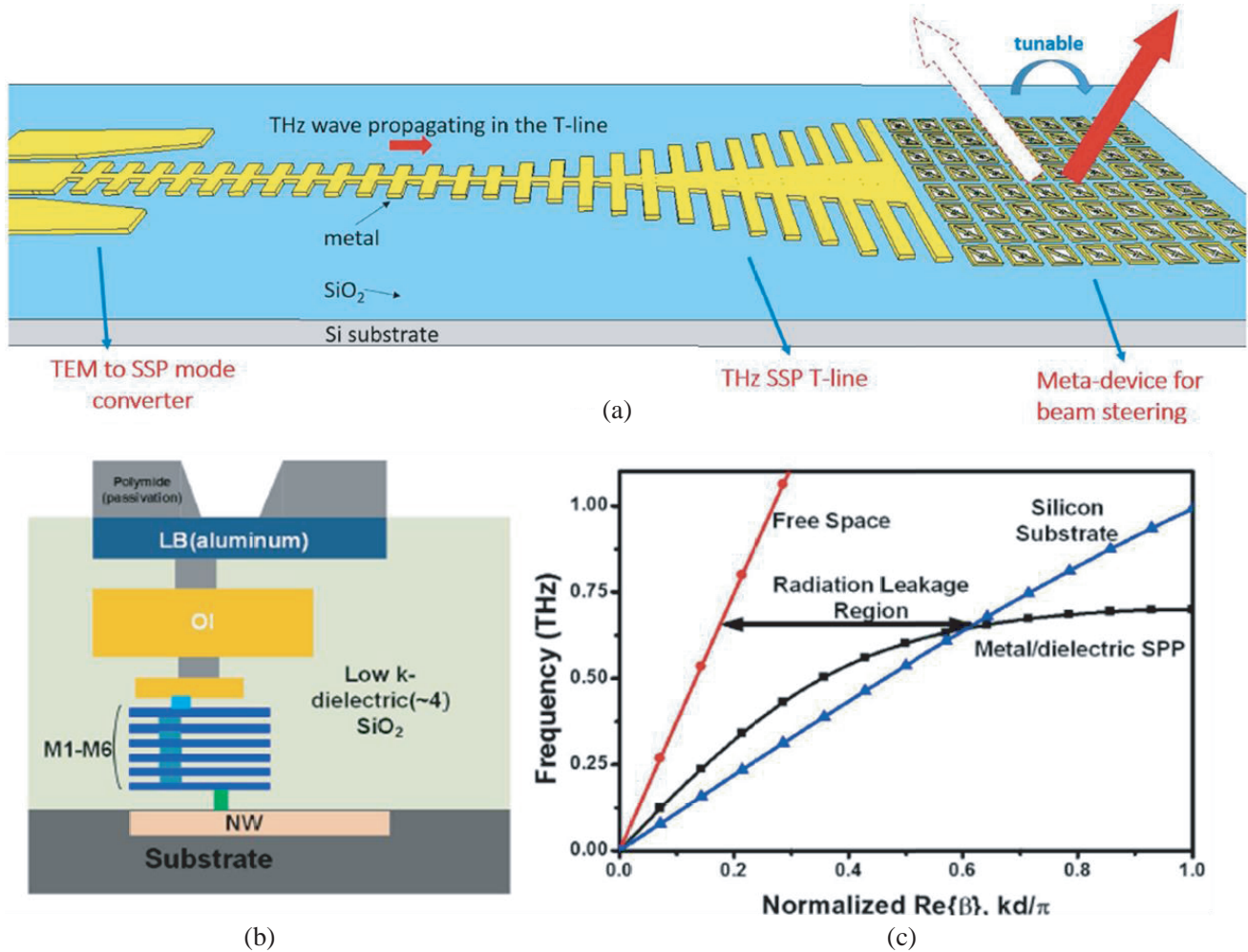
Figure 7. The structure of a CMOS THz communication I/O link [112]. (a) A CMOS THz communication I/O link, which is fed by THz spoof SPP THz transmission lines. (b) Metal configuration of back-end-of-line (BEOL) in standard 65 nm CMOS technology. (c) Simulated dispersion diagram considering the high index substrate effect.

high-density integration of memory and cores. Ref. [117] investigates the theoretical limits of the information transfer capability of spoof SPP interconnects. In the spoof SPP-based communication networks, there is a geometrically relevant trade-off between the crosstalk limited bandwidth density and information traveling length. As shown in Fig. 9, examples are given to demonstrate that the spoof SPP communication networks with a bandwidth density of 1 Gbps/µm can transmit 300 Gbps of information per channel with nominal crosstalk [117]. We observe the advantage of miniaturization of the spoof SPP interconnects compared to other interconnects with the same crosstalk capability.

A compact millimeter-wave broadband bandpass filter (BPF) based on spoof SPP using the slotted half-mode substrate integrated waveguides (HMSIW) has been presented in [118], as shown in Fig. 10(a). Due to the ability of strong field confinement, the proposed on-chip spoof SPP structure has lower coupling characteristics to dense transmission line circuits than conventional HMSIW structures. The coupling between the proposed spoof SPP structure and microstrip line is obviously weaker than its counterpart HMSIW case within the passband frequency range of $55.6 \sim 79.4$ GHz. The maximum improvement of coupling suppression is observed at 70 GHz reaching up to 30 dB. It is helpful for reducing inter-circuit interference on the chip and in turn allows for miniaturized circuits. However, it should also be noted that its lateral dimensions can be further reduced for application in integrated circuits. In [119], a GaAs-based wideband spoof SPP waveguide with super compact size has been presented
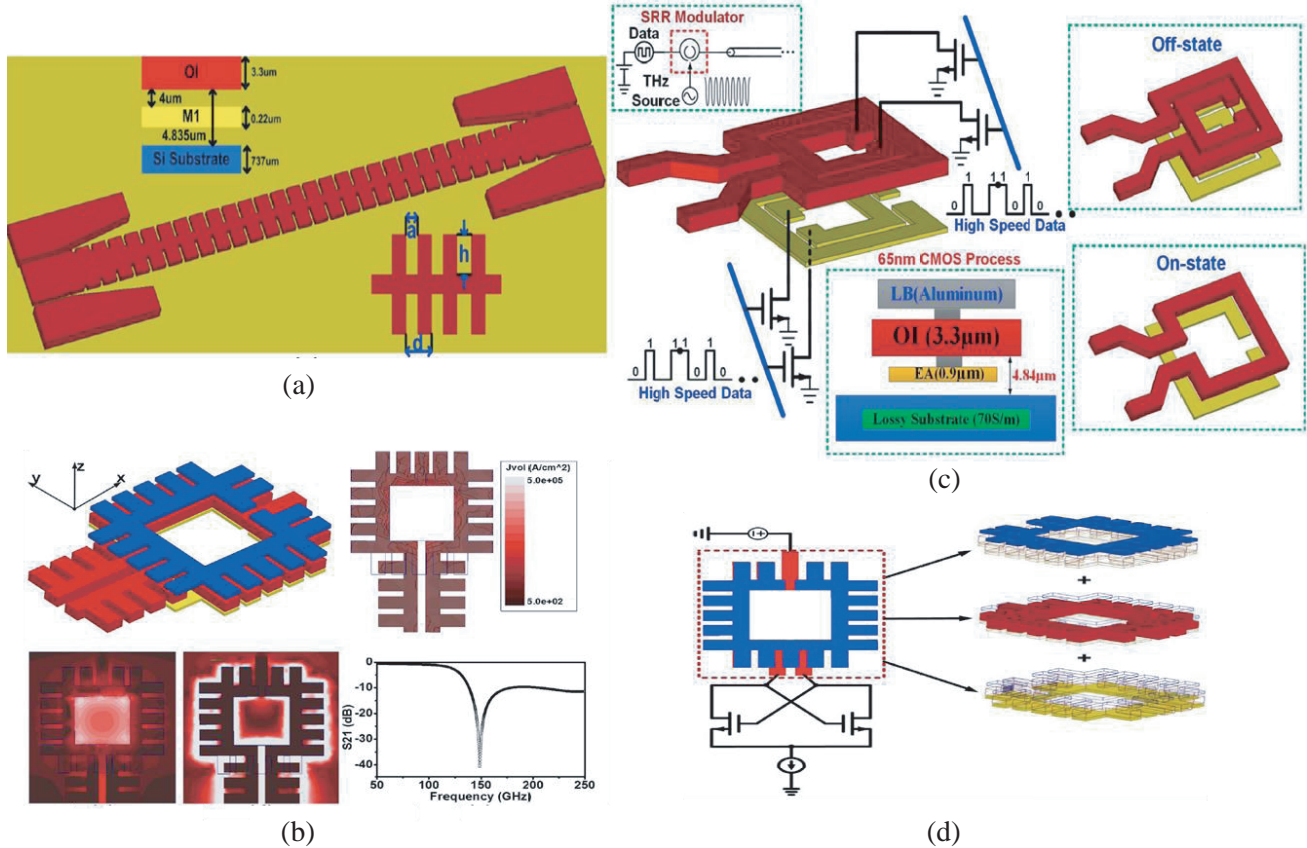
Figure 8. Spoof SPP transmission line and converter [113]. (a) The structure of spoof SPP transmission line and converter. (b) Spoof SPP modulator. (c) Spoof SPP resonator. (d) Architecture of 140-GHz fundamental surface-wave oscillator.

at millimeter-wave regime. Spoof SPP unit cells consist of a longitudinal slot and a meander slot in transverse direction, and their corresponding waveguide has good low-pass filtering features. Microstrip lines can be well matched in terms of momentum for supplying the spoof SPPs with measurement signals. Thus, the millimeter-wave on-chip BPFs with tunable center frequency and bandwidth are expected to be used in compact integrated circuits or 5G communication systems because of their broadband filtering characteristics and low coupling characteristics [118, 119].

In the conventional inductor resonators, high Q value and miniaturization cannot be achieved simultaneously [120–122]. With significant capacitive loading, the switching power amplifier modulation speed is low and occupies a large silicon area. In [123], a spoof SPP D-band signal source has been implemented, as shown in Fig. 11. A set of metal slots perpendicular to the current direction was drilled into the split-ring resonator (SRR) lanes. As a result, field-constrained slow waves are excited throughout the stacked SRR. This leads to a shorter physical length of the in-phase power synthesis, resulting in a higher quality factor and a smaller area. The four oscillator units are magnetically synchronized by the spoof SPP transmission line to form a novel coupled oscillator network (CON). The measurements show that the modulator achieves 3 dB insertion loss in the on state and 43 dB isolation in the off state, producing a 40 dB extinction ratio at 125 GHz in an area of only 40 μm ∗ 67 $upmu$m.

Although some applications in chip miniaturization utilizing the crosstalk suppression property of spoof SPPs have emerged, the potential of spoof SPP-based MICs is yet to be explored. According to some latest research on SPPs using the PCB technology, several possible future tendencies of MICs based on spoof SPPs can be predicted. The first possible tendency is the further miniaturization of transmission line structures. In [124], the contradiction between the strong field confinement and the geometric miniaturization of spoof SPP transmission lines is revealed, and zigzag grooves can be utilized
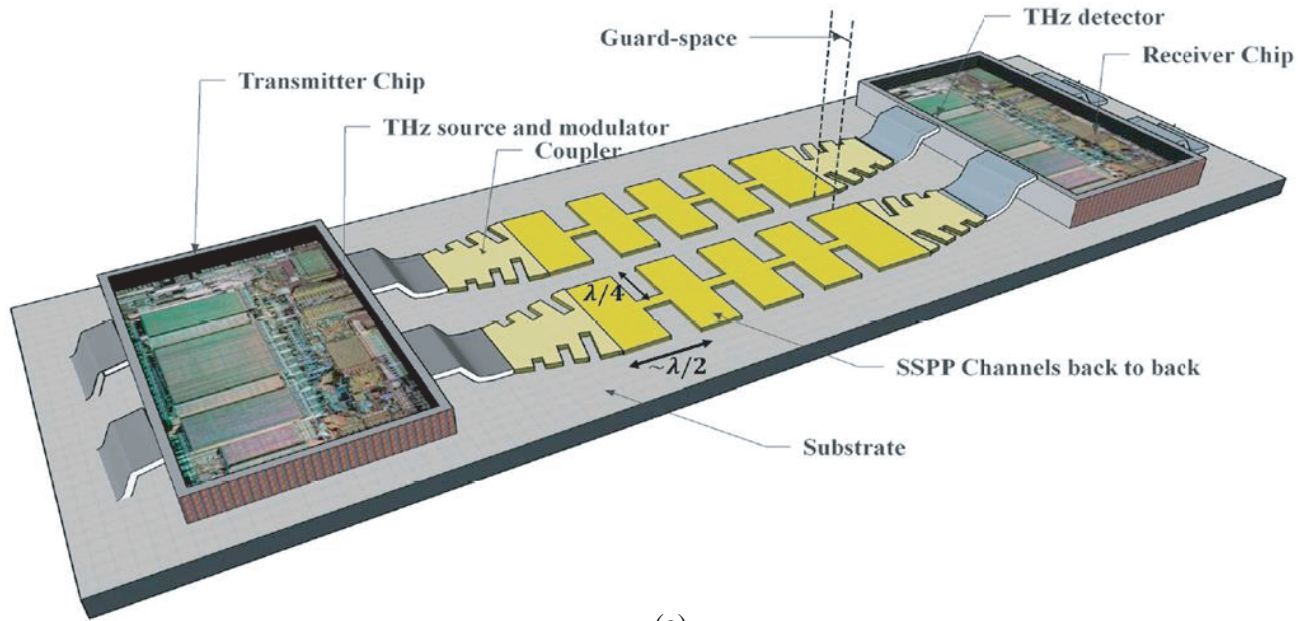
(a)
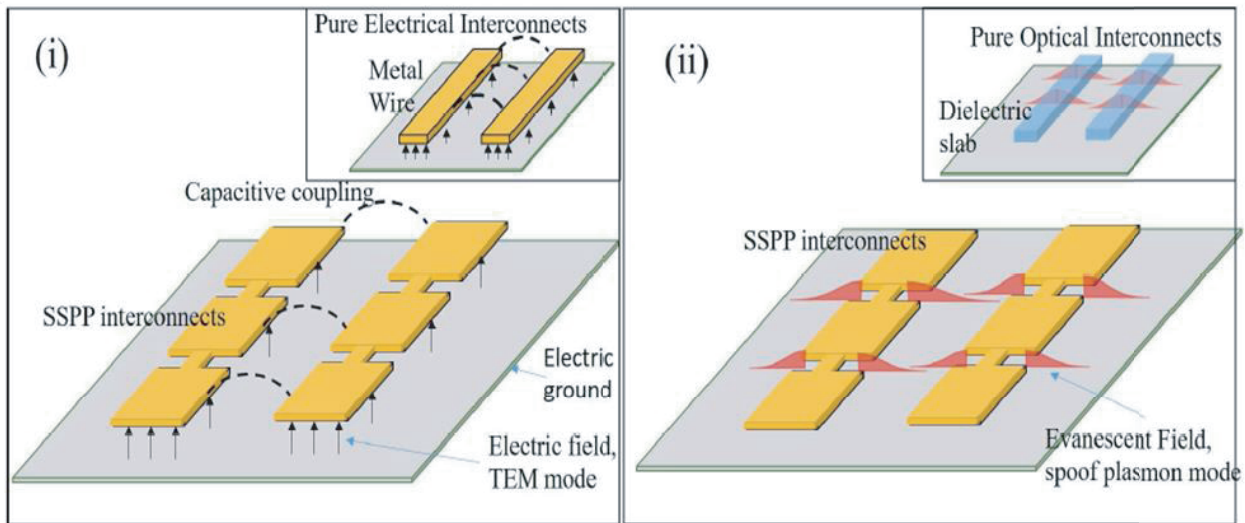
(b)

Figure 9. The spoof SPP channels [117]. (a) An inter-chip communication network employing spoof SPP channels. (b) Illustration of two different kind of modes that can be supported in spoof SPP interconnects.

to reduce the total size of the spoof SPP transmission lines. Since the reported works of on-chip spoof SPPs are mainly based on typical structures with straight slot, further miniaturization of spoof SPP transmission line structures is obviously practicable. The second tendency is the digitization of MICs based on digital spoof SPPs. Ref. [125] reported a dynamic dispersion tunable based conformal from primitives such as super surface design and implementation, as shown in Fig. 12(b). This research makes an important step for the realization of subwavelength integrated circuits. The third tendency is the systematization of spoof SPP-based MICs. Spoof SPPs make it possible to break down barrier to sub-diffraction-limit signal communication at both device and system levels. In [126], a compact planar wireless communication system with integrated spoof SPP channels can be combined with CMOS integrated circuit technology.

(a)

(b)
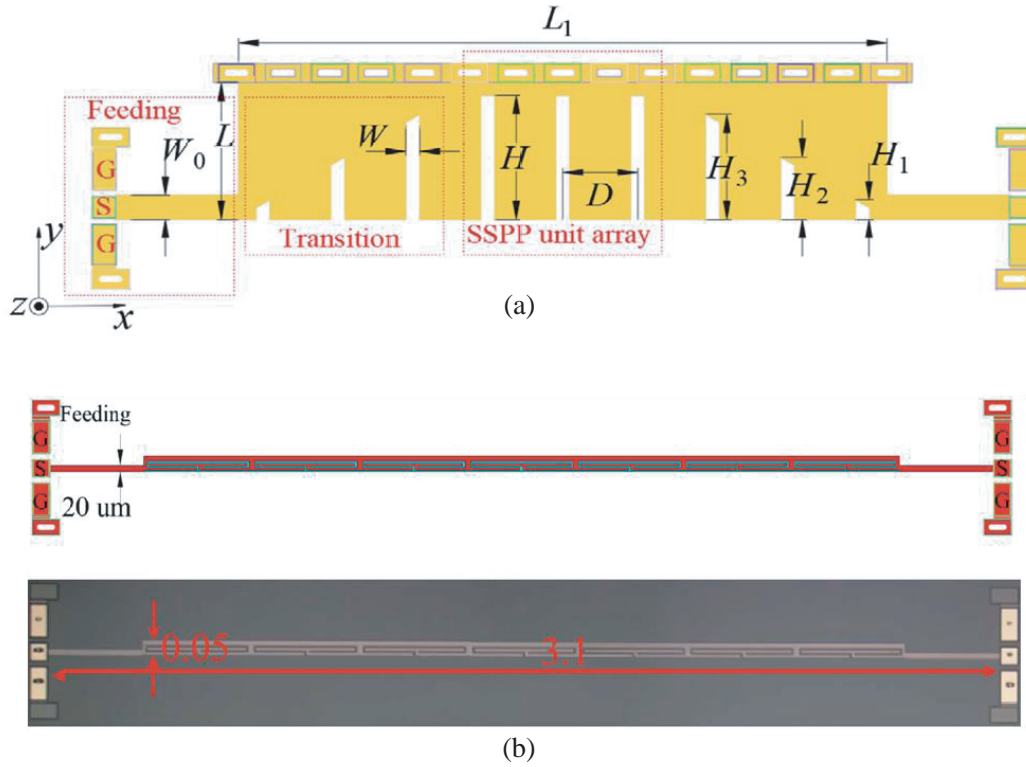
Figure 10. The spoof SPP on-chip BPFs. (a) Topology of the proposed broadband on-chip BPF [125]. (b) A GaAs-based wideband spoof SPP waveguide with super compact size [119].

(a)

(b)

(c)

Figure 11. The spoof SPP on-chip CON [123]. (a) Proposed four-way power-combined CON loaded by the proposed slow-wave resonator and spoof SPP transmission line network. (b) Die photograph of the proposed on-chip D-band modulator. (c) CON die photograph and D-band measurement setup.

(a)

(b)

(c)

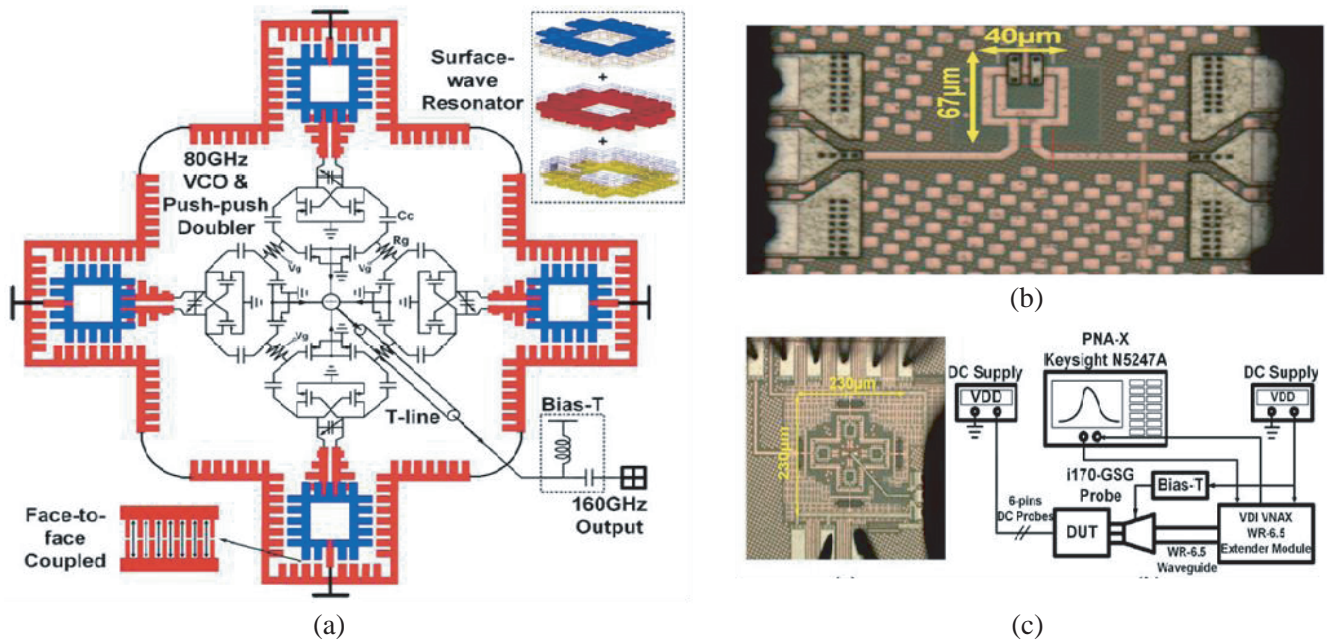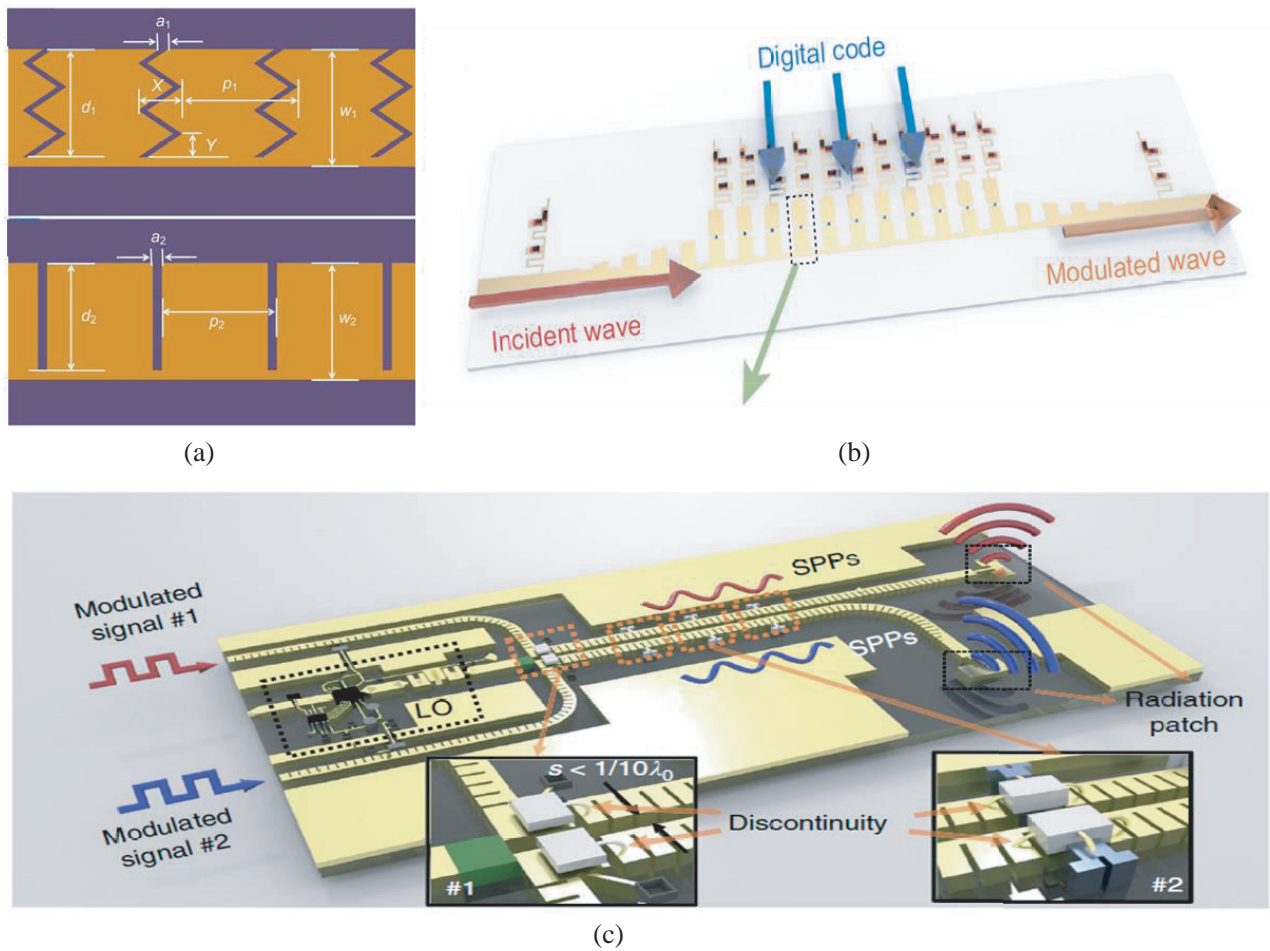**Figure 12.** The new spoof SPP transmission lines and devices. (a) The detailed geometric configuration of the new spoof SPP TL and conventional spoof SPP transmission lines [124]. (b) A schematic diagram of the prototype of the digital SPP waveguide [125]. (c) Schematic representation of the system [126].

In general, the emergence of these studies, such as spoof SPP-TLs, I/O interconnects, bandpass filters, and coupled oscillators, is conducive to resolving the contradiction between electromagnetic compatibility and miniaturization of MICs. The research on on-chip spoof SPPs is still in its infancy although some exciting results have emerged, and the ability to strongly attenuate electromagnetic crosstalk in densely integrated environments through on-chip spoof SPP has not been well revealed or explored at high frequencies. Meanwhile, the spoof SPPs based on the PCB technology has paved the future way of the on-chip spoof SPPs including further miniaturization, digitization, and systematization.

4. CONCLUSION

This paper reviews the applications of SPPs in PIC and spoof SPPs in MIC miniaturizations. For PICs based on SPPs, the SPP waveguide, including hybrid wedge plasmon polariton waveguide and gold film plasmonic waveguide, allows for small dimensions with the same other properties, which in turn promises highly integrated optical interconnects. SPPs can constitute highly integrated optical sensors that find important applications in environmental monitoring, biomedical and chemical research. In addition, the introduction of SPPs enables modern on-chip wireless communication systems at visible wavelengths, reduces losses and the number of waveguides required, and realizes miniaturization of communication systems. For MICs based on spoof SPPs, some results have been yielded, such as spoof

SPP-TLs, I/O interconnects, bandpass filters, and coupled oscillators, solving the paradoxical problem between miniaturization and electromagnetic compatibility of MICs at high frequencies. Moreover, the latest theoretical research on SPPs indicates the possible future tendency of spoof SPP-based MICs including further miniaturization, digitization, and systematization.

ACKNOWLEDGMENT

REFERENCES

1. You, X. H., C. X. Wang, J. Huang, X. Q. Gao, Z. C. Zhang, M. Wang, Y. M. Huang, C. Zhang, Y. X. Jiang, J. H. Wang, M. Zhu, B. Sheng, D. M. Wang, Z. W. Pan, P. C. Zhu, Y. Yang, Z. N. Liu, P. Zhang, X. F. Tao, S. Q. Li, Z. Chen, X. Y. Ma, C. L. I, S. F. Han, K. Li, C. K. Pan, Z. M. Zheng, L. Hanzo, X. M. Shen, Y. J. Guo, Z. G. Ding, H. Haas, W. Tong, P. Y. Zhu, G. H. Yang, J. Wang, E. G. Larsson, H. Q. Ngo, W. Hong, H. M. Wang, D. B. Hou, J. X. Chen, Z. Chen, Z. C. Hao, G. Y. Li, R. Tafazolli, Y. Gao, H. V. Poor, G. P. Fettweis, and Y. C. Liang, "Towards 6G wireless communication networks: Vision, enabling technologies, and new paradigm shifts," *Sci. China Inform. Sci.*, Vol. 64, 2021.

2. Wetzstein, G., A. Ozcan, S. Gigan, S. H. Fan, D. Englund, M. Soljacic, C. Denz, D. A. B. Miller, and D. Psaltis, "Inference in artificial intelligence with deep optics and photonics," *Nature*, Vol. 588, 39–47, 2020.

3. Alfaras, M., W. Primett, M. Umair, C. Windlin, P. Karpashevich, N. Chalabianloo, D. Bowie, C. Sas, P. Sanches, K. Hook, C. Ersoy, and H. Gamboa, "Biosensing and actuation-platforms coupling body input-output modalities for affective technologies," *Sensors-Basel*, Vol. 20, 2020.

4. Koos, C., W. Freude, J. Leuthold, M. Kohl, L. R. Dalton, W. Bogaerts, M. Lauermann, S. Wolf, C. Weimann, A. Melikyan, N. Lindenmann, M. R. Billah, S. Muehlbrandt, S. Koeber, R. Palmer, K. Koehnle, L. Alloatti, D. L. Elder, A. L. Giesecke, T. Wahlbrink, and IEEE, "Silicon-Organic Hybrid (SOH) integration and photonic multi-chip systems: Extending the capabilities of the silicon photonic platform," *IEEE Photonics Conference*, Reston, VA, 2015.

5. Ben Ahmed, A. and A. Ben Abdallah, "Hybrid silicon-photonic network-on-chip for future generations of high-performance many-core systems," *Journal of Supercomputing*, Vol. 71, 4446–4475, 2015.

6. Gadot, F., T. Brillat, E. Akmansoy, and A. de Lustrac, "New type of metallic photonic bandgap material suitable for microwave applications," *Electron. Lett.*, Vol. 36, 640–641, 2000.

7. Garenaux, K., T. Merlet, M. Alouini, J. Lopez, N. Vodjdani, and R. Boula-Picard, "Recent breakthroughs in RF photonics for radar systems," *IEEE Aerospace and Electronic Systems Magazine*, Vol. 22, 3–8, 2007.

8. Arai, Y., M. Sato, H. T. Yamada, T. Hamada, K. Nagai, and H. I. Fujishiro, "60-GHz flip-chip assembled MIC design considering chip-substrate effect," *IEEE Transactions on Microwave Theory and Techniques*, Vol. 45, 2261–2266, 1997.

9. Miyashita, D., S. Kousai, T. Suzuki, and J. Deguchi, "A neuromorphic chip optimized for deep learning and CMOS technology with time-domain analog and digital mixed-signal processing," *IEEE J. Solid-State Circuits*, Vol. 52, 2679–2689, 2017.

10. Qian, G., K. Qian, X. Gu, Y. Kong, and T. Chen, "Integrated chip technologies for microwave photonics," *Journal of Radars*, Vol. 8, 262–280, 2019.

11. Wang, Z., X. Jia, H. Wu, F. Peng, Y. Fu, Y. Rao, and IEEE, 'Towards ultra-long-distance distributed fiber-optic sensing," *25th International Conference on Optical Fibre Sensors (OFS)*, South Korea, 2017.

12. Galas, J., D. Litwin, N. Blocki, and M. Daszkiewicz, "Photonic technology revolution influence on the defence area," *Conference on Electro-Optical Remote Sensing XI*, Warsaw, Poland, 2017.

13. Lee, E.-H., "VLSI photonic interconnection of dielectric and plasmonic nano-wires and devices," *13th International Conference on Transparent Optical Networks (ICTON)*, Stockholm, Sweden, 2011.

14. Zhang, W. and J. Yao, "Silicon photonic integrated optoelectronic oscillator for frequency-tunable microwave generation," *J. Lightwave Technol.*, Vol. 36, 4655–4663, 2018.

15. Yuan, X. G., Y. Yang, X. Yan, Y. A. Zhang, and X. Zhang, "Ultra-compact multichannel optical waveguide crossings designed by a particle swarm optimized method," *Opt. Commun.*, Vol. 503, 2022.

16. Leslie, M., "Light-based chips promise to slash energy use and increase speed," *Engineering*, Vol. 7, 1195–1196, 2021.

17. Moss, D., "11 Tera-FLOP/s photonic convolutional accelerator for optical neural networks," *Center for Open Science*, 2021.

18. Liu, Y., K. Xu, S. Wang, W. Shen, H. Xie, Y. Wang, S. Xiao, Y. Yao, J. Du, Z. He, and Q. Song, "Arbitrarily routed mode-division multiplexed photonic circuits for dense integration," *Nat. Commun.*, Vol. 10, 2019.

19. Torres, J. P. and J. C. Freire, "MMIC chips on board for wireless communications," *4th International Conference on Millimeter and Submillimeter Waves and Applications*, 112–116, San Diego, CA, 1998.

20. Branch, J., X. Guo, L. Gao, A. Sugavanam, J. J. Lin, and K. K. O, "Wireless communication in a flip-chip package using integrated antennas on silicon substrates," *IEEE Electron Device Lett.*, Vol. 26, 115–117, 2005.

21. Wu, Y. L., M. D. Kong, Z. Zhuang, and W. M. Wang, "Creating distinctive connections between multifunctional microwave circuits and mobile-terminal radio-frequency integrated chips using integrated passive device technology," *China Communications*, Vol. 18, 121–132, 2021.

22. Lee, S. K., B. Kim, H. J. Park, and J. Y. Sim, "A 5 Gb/s single-ended parallel receiver with adaptive crosstalk-induced jitter cancellation," *IEEE J. Solid-State Circuits*, Vol. 48, 2118–2127, 2013.

23. Smith, H., A. Deutsch, S. Mehrotra, D. Widiger, M. Bowen, A. Dansky, G. Kopcsay, B. Krauter, and I. IEEE, "Frequency dependent RLC crosstalk evaluation of a high performance S/390 microprocessor chip," *9th IEEE Topical Meeting on Electrical Performance of Electronic Packaging*, 321–324, Scottsdale, Az, 2000.

24. Lee, G. A., H. Y. Lee, and IEEE, "Suppression of leakage and crosstalk in typical millimeter-wave flip-chip packages," *6th Topical Meeting on Electrical Performance of Electronic Packaging*, 195–198, San Jose, CA, 1997.

25. Wen, X. M., Y. G. Bi, F. S. Yi, X. L. Zhang, Y. F. Liu, W. Q. Wang, J. Feng, and H. B. Sun, "Tunable surface plasmon-polariton resonance in organic light-emitting devices based on corrugated alloy electrodes," *Opto-Electronic Advances*, Vol. 4, 2021.

26. Barnes, W. L., A. Dereux, and T. W. Ebbesen, "Surface plasmon subwavelength optics," *Nature*, Vol. 424, 824–830, 2003.

27. Fang, N., H. Lee, C. Sun, and X. Zhang, "Sub-diffraction-limited optical imaging with a silver superlens," *Science*, Vol. 308, 534–537, 2005.

28. Chen, Q., L. Liang, Q. L. Zheng, Y. X. Zhang, and L. Wen, "On-chip readout plasmonic mid-IR gas sensor," *Opto-Electronic Advances*, Vol. 3, 2020.

29. Hu, A. Q., S. Liu, J. Y. Zhao, T. Wen, W. D. Zhang, Q. H. Gong, Y. Q. Meng, Y. Ye, and G. W. Lu, "Controlling plasmon-exciton interactions through photothermal reshaping," *Opto-Electronic Advances*, Vol. 3, 2020.

30. Jones, A. C., R. L. Olmon, S. E. Skrabalak, B. J. Wiley, Y. N. Xia, and M. B. Raschke, "Mid-IR plasmonics: Near-field imaging of coherent plasmon modes of silver nanowires," *Nano Lett.*, Vol. 9, 2553, 2009.

31. Zhang, L., Z. Chen, K. Zhang, L. Wang, H. Xu, L. Han, W. Guo, Y. Yang, C.-N. Kuo, C. S. Lue, D. Mondal, J. Fuji, I. Vobornik, B. Ghosh, A. Agarwal, H. Xing, X. Chen, A. Politano, and W. Lu, "High-frequency rectifiers based on type-II Dirac fermions," *Nat. Commun.*, Vol. 12, 2021.

32. Zhang, L., C. Guo, C.-N. Kuo, H. Xu, K. Zhang, B. Ghosh, J. De Santis, D. W. Boukhvalov, I. Vobornik, V. Paolucci, C. S. Lue, H. Xing, A. Agarwal, L. Wang, and A. Politano, "Terahertz photodetection with Type-II Dirac fermions in transition-metal ditellurides and their heterostructures," *Physica Status Solidi (RRL) — Rapid Research Letters*, Vol. 15, 2100212, 2021.

33. Wang, L., L. Han, W. Guo, L. Zhang, C. Yao, Z. Chen, Y. Chen, C. Guo, K. Zhang, C.-N. Kuo, C. S. Lue, A. Politano, H. Xing, M. Jiang, X. Yu, X. Chen, and W. Lu, "Hybrid Dirac semimetal-based photodetector with efficient low-energy photon harvesting," *Light: Science & Amp. Applications*, Vol. 11, 2022.

34. Viti, L., D. Coquillat, A. Politano, K. A. Kokh, Z. S. Aliev, M. B. Babanly, O. E. Tereshchenko, W. Knap, E. V. Chulkov, and M. S. Vitiello, "Plasma-wave terahertz detection mediated by topological insulators surface states," *Nano Lett.*, Vol. 16, 80–87, 2015.

35. Mitrofanov, O., L. Viti, E. Dardanis, M. C. Giordano, D. Ercolani, A. Politano, L. Sorba, and M. S. Vitiello, "Near-field terahertz probes with room-temperature nanodetectors for subwavelength resolution imaging," *Sci. Rep. — UK*, Vol. 7, 2017.

36. Pogna, E. A. A., L. Viti, A. Politano, M. Brambilla, G. Scamarcio, and M. S. Vitiello, "Mapping propagation of collective modes in Bi2Se3 and Bi2Te2.2Se0.8 topological insulators by near-field terahertz nanoscopy," *Nat. Commun.*, Vol. 12, 2021.

37. Agarwal, A., M. S. Vitiello, L. Viti, A. Cupolillo, and A. Politano, "Plasmonics with two-dimensional semiconductors: From basic research to technological applications," *Nanoscale*, Vol. 10, 8938–8946, 2018.

38. Politano, A. and G. Chiarello, "Plasmon modes in graphene: Status and prospect," *Nanoscale*, Vol. 6, 10927–10940, 2014.

39. Bao, Q. and K. P. Loh, "Graphene photonics, plasmonics, and broadband optoelectronic devices," *ACS Nano*, Vol. 6, 3677–3694, 2012.

40. Low, T. and P. Avouris, "Graphene plasmonics for terahertz to mid-infrared applications," *ACS Nano*, Vol. 8, 1086–1101, 2014.

41. Stauber, T., "Plasmonics in Dirac systems: From graphene to topological insulators," *J. Phys.: Condens. Matter*, Vol. 26, 123201, 2014.

42. Politano, A., V. M. Silkin, I. A. Nechaev, M. S. Vitiello, L. Viti, Z. S. Aliev, M. B. Babanly, G. Chiarello, P. M. Echenique, and E. V. Chulkov, "Interplay of surface and dirac plasmons in topological insulators: The case of Bi_2Se_3," *Phys. Rev. Lett.*, Vol. 115, 2015.

43. Politano, A., L. Viti, and M. S. Vitiello, "Optoelectronic devices, plasmonics, and photonics with topological insulators," *Apl. Mater.*, Vol. 5, 035504, 2017.

44. Sadhukhan, K., A. Politano, and A. Agarwal, "Novel undamped gapless plasmon mode in a tilted Type-II Dirac semimetal," *Phys. Rev. Lett.*, Vol. 124, 2020.

45. Politano, A., H. K. Yu, D. Farías, and G. Chiarello, "Multiple acoustic surface plasmons in graphene/Cu(111) contacts," *Phys. Rev. B*, Vol. 97, 2018.

46. Dutta, D., B. Ghosh, B. Singh, H. Lin, A. Politano, A. Bansil, and A. Agarwal, "Collective plasmonic modes in the chiral multifold fermionic material CoSi," *Phys. Rev. B*, Vol. 105, 2022.

47. Politano, A., A. R. Marino, V. Formoso, D. Farías, R. Miranda, and G. Chiarello, "Evidence for acoustic-like plasmons on epitaxial graphene on Pt(111)," *Phys. Rev. B*, Vol. 84, 2011.

48. Chiarello, G., J. Hofmann, Z. Li, V. Fabio, L. Guo, X. Chen, S. Das Sarma, and A. Politano, "Tunable surface plasmons in Weyl semimetals TaAs and NbAs," *Phys. Rev. B*, Vol. 99, 2019.

49. Schuller, J. A., E. S. Barnard, W. S. Cai, Y. C. Jun, J. S. White, and M. L. Brongersma, "Plasmonics for extreme light concentration and manipulation," *Nat. Mater.*, Vol. 9, 193–204, 2010.

50. Pendry, J. B., L. Martin-Moreno, and F. J. Garcia-Vidal, "Mimicking surface plasmons with structured surfaces," *Science*, Vol. 305, 847–848, 2004.

51. Hibbins, A. P., B. R. Evans, and J. R. Sambles, "Experimental verification of designer surface plasmons," *Science*, Vol. 308, 670–672, 2005.

52. Yu, N. F., Q. J. Wang, M. A. Kats, J. A. Fan, S. P. Khanna, L. H. Li, A. G. Davies, E. H. Linfield, and F. Capasso, "Designer spoof surface plasmon structures collimate terahertz laser beams," *Nat. Mater.*, Vol. 9, 730–735, 2010.

53. Kats, M. A., D. Woolf, R. Blanchard, N. F. Yu, and F. Capasso, "Spoof plasmon analogue of metal-insulator-metal waveguides," *Opt. Express*, Vol. 19, 14860–14870, 2011.

54. Woolf, D., M. A. Kats, and F. Capasso, "Spoof surface plasmon waveguide forces," *Opt. Lett.*, Vol. 39, 517–520, 2014.

55. Erementchouk, M., S. R. Joy, and P. Mazumder, "Electrodynamics of spoof plasmons in periodically corrugated waveguides," *Proceedings of the Royal Society A — Mathematical Physical and Engineering Sciences*, Vol. 472, 2016.

56. Zhang, H. C., P. H. He, Z. X. Liu, W. X. Tang, A. Aziz, J. Xu, S. Liu, X. Y. Zhou, and T. J. Cui, "Dispersion analysis of deep-subwavelength-decorated metallic surface using field-network joint solution," *IEEE Transactions on Antennas and Propagation*, Vol. 66, 2923–2933, 2018.

57. Zhang, H. C., P. H. He, X. X. Gao, J. Y. Lu, T. J. Cui, and Y. Luo, "Loss analysis of plasmonic metasurfaces using field-network-joint method," *IEEE Transactions on Antennas and Propagation*, Vol. 67, 3521–3526, 2019.

58. He, P. H., L. Y. Niu, Y. Fan, H. C. Zhang, L. P. Zhang, D. Y. Yao, W. X. Tang, and T. J. Cui, "Active odd-mode-metachannel for single-conductor systems," *Opto-Electronic Advances*, Vol. 5, 210119–210119, 2022.

59. Shen, X. P., T. J. Cui, D. Martin-Cano, and F. J. Garcia-Vidal, "Conformal surface plasmons propagating on ultrathin and flexible films," *Proc. Natl. Acad. Sci. U. S. A.*, Vol. 110, 40–45, 2013.

60. Shen, X. P. and T. J. Cui, "Planar plasmonic metamaterial on a thin film with nearly zero thickness," *Applied Physics Letters*, Vol. 102, 2013.

61. Barnes, W. L., "Surface plasmon-polariton length scales: A route to sub-wavelength optics," *J. Opt. A — Pure Appl. Op.*, Vol. 8, S87–S93, 2006.

62. Zia, R., J. A. Schuller, A. Chandran, and M. L. Brongersma, "Plasmonics: The next chip-scale technology," *Materials Today*, Vol. 9, 20–27, 2006.

63. Meng, Y., Y. Z. Chen, L. H. Lu, Y. M. Ding, A. Cusano, J. A. Fan, Q. M. Hu, K. Y. Wang, Z. W. Xie, Z. T. Liu, Y. M. Yang, Q. Liu, M. L. Gong, Q. R. Xiao, S. L. Sun, M. M. Zhang, X. C. Yuan, and X. J. Ni, "Optical meta-waveguides for integrated photonics and beyond," *Light-Sci. Appl.*, Vol. 10, 2021.

64. Pile, D. F. P., T. Ogawa, D. K. Gramotnev, Y. Matsuzaki, K. C. Vernon, K. Yamaguchi, T. Okamoto, M. Haraguchi, and M. Fukui, "Two-dimensionally localized modes of a nanoscale gap plasmon waveguide," *Appl. Phys. Lett.*, Vol. 87, 261114, 2005.

65. Liu, L., Z. Han, and S. He, "Novel surface plasmon waveguide for high integration," *Opt. Express*, Vol. 13, 6645–6650, 2005.

66. Dionne, J. A., L. A. Sweatlock, H. A. Atwater, and A. Polman, "Plasmon slot waveguides: Towards chip-scale propagation with subwavelength-scale localization," *Phys. Rev. B*, Vol. 73, 035407, 2006.

67. Ajoy, A., Y. X. Liu, K. Saha, L. Marseglia, J. C. Jaskula, U. Bissbort, and P. Cappellaro, "Quantum interpolation for high-resolution sensing," *Proc. Natl. Acad. Sci. U. S. A.*, Vol. 114, 2149, 2017.

68. Istrate, E. and E. H. Sargent, "Photonic crystal heterostructures and interfaces," *Rev. Mod. Phys.*, Vol. 78, 455, 2006.

69. Liu, L., Z. Han, and S. He, "Novel surface plasmon waveguide for high integration," *Opt. Express*, Vol. 13, 6645, 2005.

70. Oulton, R. F., V. J. Sorger, D. A. Genov, D. F. P. Pile, and X. Zhang, "A hybrid plasmonic waveguide for subwavelength confinement and long-range propagation," *Nature Photonics*, Vol. 2, 496–500, 2008.

71. Bian, Y. S., Z. Zheng, Y. Liu, J. S. Zhu, and T. Zhou, "Dielectric-loaded surface plasmon polariton waveguide with a holey ridge for propagation-loss reduction and subwavelength mode confinement," *Opt. Express*, Vol. 18, 23756–23762, 2010.

72. Avrutsky, I., R. Soref, and W. Buchwald, "Sub-wavelength plasmonic modes in a conductor-gap-dielectric system with a nanoscale gap," *Opt. Express*, Vol. 18, 348–363, 2010.

73. Bian Y. S., Z. Zheng, Y. Liu, J. S. Zhu, and T. Zhou, "Hybrid wedge plasmon polariton waveguide with good fabrication-error-tolerance for ultra-deep-subwavelength mode confinement," *Opt. Express*, Vol. 19, 22417–22422, 2011.

74. Oulton, R. F., V. J. Sorger, D. A. Genov, D. F. P. Pile, and X. Zhang, "A hybrid plasmonic waveguide for subwavelength confinement and long-range propagation," *Nature Photonics*, Vol. 2, 496–500, 2008.

75. Oulton, R. F., V. J. Sorger, T. Zentgraf, R. M. Ma, C. Gladden, L. Dai, G. Bartal, and X. Zhang, "Plasmon lasers at deep subwavelength scale," *Nature*, Vol. 461, 629–632, 2009.

76. Bian, Y., Z. Zheng, Y. Liu, J. Zhu, and T. Zhou, "Coplanar plasmonic nanolasers based on edge-coupled hybrid plasmonic waveguides," *IEEE Photonics Technol. Lett.*, Vol. 23, 884–886, 2011.

77. Zhang, X. Y., A. Hu, J. Z. Wen, T. Zhang, X. J. Xue, Y. Zhou, and W. W. Duley, "Numerical analysis of deep sub-wavelength integrated plasmonic devices based on semiconductor-insulator-metal strip waveguides," *Opt. Express*, Vol. 18, 18945–18959, 2010.

78. Chu, H. S., E. P. Li, P. Bai, and R. Hegde, "Optical performance of single-mode hybrid dielectric-loaded plasmonic waveguide-based components," *Appl. Phys. Lett.*, Vol. 96, 221103, 2010.

79. Wu, M., Z. H. Han, and V. Van, "Conductor-gap-silicon plasmonic waveguides and passive components at subwavelength scale," *Opt. Express*, Vol. 18, 11728–11736, 2010.

80. Fukuhara, M., M. Ota, A. Takeda, T. Aihara, H. Sakai, Y. Ishii, and M. Fukuda, "Surface-plasmon waveguides as transmission lines for optical signal and electrical bias," *IEEE J. Lightw. Technol.*, Vol. 32, 3888–8724, 2014.

81. Rakhshani, M. R. and M. A. Mansouri-Birjandi, "Dual wavelength demultiplexer based on metal-insulator-metal plasmonic circular ring resonators," *J. Mod. Opt.*, Vol. 63, 1078–1086, 2016.

82. Ding, K., M. T. Hill, Z. C. Liu, L. J. Yin, P. J. Veldhoven, and C. Z. Ning, "Record performance of electrical injection sub-wavelength metallic-cavity semiconductor lasers at room temperature," *Opt. Exp.*, Vol. 21, 4728–4733, 2013.

83. Cho, C.-H., C. O. Aspetti, J. Park, and R. Agarwal, "Silicon coupled with plasmon nanocavities generates bright visible hot luminescence," *Nature Photon.*, Vol. 7, 285–289, 2013.

84. Berini, P., "Surface plasmon photodetectors and their applications," *Laser Photon. Rev.*, Vol. 8, 197–220, 2014.

85. Ishii, T., J. Fujikata, K. Makita, T. Baba, and K. Ohashi, "Si Nano-photodiode with a surface plasmon antenna," *Jpn. J. Appl. Phys.*, Vol. 44, 364–366, 2005.

86. Melikyan, A., L. Alloatti, A. Muslija, D. Hillerkuss, P. C. Schindler, J. Li, R. Palmer, D. Korn, S. Muehlbrandt, D. Van Thourhout, B. Chen, R. Dinu, M. Sommer, C. Koos, M. Kohl, W. Freude, and J. Leuthold, "High-speed plasmonic phase modulators," *Nature Photon.*, Vol. 8, 229–233, 2014.

87. Zhu,S., G. Q. Lo, and D. L. Kwong, "Theoretical investigation of silicon MOS-type plasmonic slot waveguide based MZI modulators" *Opt. Exp.*, Vol. 18, 27802–27819, 2010.

88. Fukuhara, M., M. Ota, H. Sakai, T. Aihara, Y. Ishii, and M. Fukuda, "Low-loss waveguiding and detection structure for surface plasmon polaritons," *Appl. Phys. Lett.*, Vol. 104, 081111, 2014.

89. Aihara T., H. Sakai, A. Takeda, S. Okahisa, M. Fukuhara, M. Ota, Y. Ishii, and M. Fukuda, "Coherent plasmonic interconnection in silicon-based electrical circuit," *J. Lightwave Technol.*, Vol. 33, 2139–2145, 2015.

90. Nehl, C. L., H. Liao, and J. H. Hafner, "Optical properties of star-shaped gold nanoparticles," *Nano Lett.*, Vol. 6, 683–688, 2006.

91. Joshi, G. K., K. N. Blodgett, B. B. Muhoberac, M. A. Johnson, K. A. Smith, and R. Sardar, "Ultrasensitive photoreversible molecular sensors of azobenzene-functionalized plasmonic nanoantennas," *Nano Lett.*, Vol. 14, 532–540, 2014.

92. Liu, N., M. L. Tang, M. Hentschel, H. Giessen, and A. P. Alivisatos, "Nanoantenna-enhanced gas sensing in a single tailored nanofocus," *Nat. Mater.*, Vol. 10, 631–636, 2011.

93. Zeng, B., Y. Gao, and F. J. Bartoli, "Rapid and highly sensitive detection using Fano resonances in ultrathin plasmonicnanogratings," *Appl. Phys. Lett.*, Vol. 105, 161106, 2014.

94. Zijlstra, P., P. M. R. Paulo, and M. Orrit, "Optical detection of single non-absorbing molecules using the surface plasmon resonance of a gold nanorod," *Nat. Nanotechnol.*, Vol. 7, 379–382, 2012.

95. Lesuffleur, A., H. Im, N. C. Lindquist and S.-H. Oh, "Periodic nanohole arrays with shape-enhanced plasmon resonance as real-time biosensors," *Appl. Phys. Lett.*, Vol. 90, 243110, 2007.

96. Wang, Y. J., J. J. Chen, C. W. Sun, K. X. Rong, H. Li, and Q. H. Gong, "An ultrahigh-contrast and broadband on-chip refractive index sensor based on a surface-plasmon-polariton interferometer," *Analyst*, Vol. 140, 207890, 2015.

97. Novotny, L. and N. van Hulst, "Antennas for light," *Nat. Photonics.*, Vol. 5, 83–90, 2011.

98. Gleb, M. A., C. Argyropoulos, T. B. Hoang, C. Ciracì, C. Fang, J. Huang, D. R. Smith, and M. H. Mikkelsen, "Probing the mechanisms of large Purcell enhancement in plasmonic nanoantennas," *Nat. Photonics.*, Vol. 8, 835–840, 2014.

99. Merlo, J. M., N. T. Nesbitt, Y. M. Calm, A. H. Rose, L. D'Imperio, C. Yang, J. R. Naughton, M. J. Burns, K. Kempa, and M. J. Naughton, "Wireless communication system via nanoscale plasmonic antennas," *Sci. Rep.*, Vol. 6, 31710, 2016.

100. Heni, W., B. Baeuerle, H. Mardoyan, F. Jorge, J. M. Estaran, A. Konczykowska, M. Riet, B. Duval, V. Nodjiadjim, M. Goix, J. Y. Dupuy, M. Destraz, C. Hoessbacher, Y. Fedoryshyn, H. J. Xu, D. L. Elder, L. R. Dalton, J. Renaudier, and J. Leuthold, "Ultra-high-speed 2 : 1 digital selector and plasmonic modulator IM/DD transmitter operating at 222 GBaud for intra-datacenter applications," *Lightwave Technol.*, Vol. 38, 2734–2739, 2020.

101. Atabaki1, A. H., S. Moazeni, F. Pavanello, H. Gevorgyan, J. Notaros, L. Alloatti, M. T. Wade, C. Sun, S. A. Kruger, H. Meng, K. A. Qubaisi, I. Wang, B. Zhang, A. Khilo, C. V. Baiocco, M. Popović, V. M. Stojanović, and R. J. Ram, "Integrating photonics with silicon nanoelectronics for the next generation of systems on a chip," *Nature*, Vol. 556, 349–354, 2018.

102. Stojanović, L., R. J. Ram, M. Popović, S. Lin, S. Moazeni, M. Wade, C. Sun, L. Alloatti, A. Atabaki, F. Pavanello, N. Mehta, and P. Bhargava, "Monolithic silicon-photonic platforms in state-of-the-art CMOS SOI processes," *Opt. Express*, Vol. 26, 13106–13121, 2018.

103. Weeber, J. C., J. Arocas, O. Heintz, L. Markey, S. Viarbitskaya, G. Colas-des-Francs, K. Hammani, A. Dereux, C. Hoessbacher, U. Koch, J. Leuthold, K. Rohracher, A. L. Giesecke, C. Porschatis, T. Wahlbrink, B. Chmielak, N. Pleros, and D. Tsiokos, "Characterization of CMOS metal based dielectric loaded surface plasmon waveguides at telecom wavelengths," *Opt. Express*, Vol. 25, 394–408, 2017.

104. Ueli, K., C. Uhl, H. Hettrich, Y. Fedoryshyn, C. Hoessbacher, W. Heni, B. Baeuerle, B. I. Bitachon, A. Josten, M. Ayata, H. Xu, D. L. Elder, L. R. Dalton, E. Mentovich, P. Bakopoulos, S. Lischke, A. Krüger, L. Zimmermann, D. Tsiokos, N. Pleros, M. Möller, and J. Leuthold, "A monolithic bipolar CMOS electronic-plasmonic high-speed transmitter," *Nat. Electron.*, Vol. 3, 338–345, 2020.

105. Zhou, Y. J., Q. Jiang, and T. J. Cui, "Bidirectional bending splitter of designer surface plasmons," *Applied Physics Letters*, Vol. 99, 111904, 2011.

106. Nazari, M. H. and A. E. Neyestanak, "A 15-Gb/s 0.5-mW/Gbps two-tap DFE receiver with far-end crosstalk cancellation," *IEEE J. Solid-State Circuits*, Vol. 47, 2420–2432, 2012.

107. Liang, Y., H. Yu, H. C. Zhang, C. Yang, and T. J. Cui, "On-chip sub-terahertz surface plasmon polariton transmission lines in CMOS," *Sci. Rep. — UK*, Vol. 5, 2015.

108. Liang, Y., H. Yu, J. Zhao, W. Yang, and Y. Wang, "An energy efficient and low cross-talk CMOS sub-THz I/O with surface-wave modulator and interconnect," presented at the *2015 IEEE/ACM International Symposium on Low Power Electronics and Design (ISLPED)*, July 2015.

109. Ma, H. F., X. P. Shen, Q. Cheng, W. X. Jiang, and T. J. Cui, "Broadband and high-efficiency conversion from guided waves to spoof surface plasmon polaritons," *Laser & Photonics Reviews*, Vol. 8, 146–151, 2014.

110. Kianinejad, A., Z. N. Chen, and C. W. Qiu, "Design and modeling of spoof surface plasmon modes-based microwave slow-wave transmission line," *IEEE Transactions on Microwave Theory and Techniques*, Vol. 63, 1817–1825, 2015.

111. Yan, R. T., H. C. Zhang, P. H. He, Z. X. Wang, X. Zhang, X. Fu, and T. J. Cui, "A broadband and high-efficiency compact transition from microstrip line to spoof surface plasmon polaritons," *IEEE Microwave and Wireless Components Letters*, Vol. 30, 23–26, 2020.

112. Liang, Y., H. Yu, J. C. Wen, A. A. A. Apriyana, N. Li, Y. Luo, and L. L. Sun, "On-chip sub-terahertz surface plasmon polariton transmission lines with mode converter in CMOS," *Sci. Rep. — UK*, Vol. 6, 2016.

113. Liang, Y., H. Yu, G. Y. Feng, A. A. A. Apriyana, X. J. Fu, and T. J. Cui, "An energy-efficient and low-crosstalk sub-THz I/O by surface plasmonic polariton interconnect in CMOS," *IEEE Transactions on Microwave Theory and Techniques*, Vol. 65, 2762–2774, 2017.

114. Young, I. A., E. Mohammed, J. T. S. Liao, A. M. Kern, S. Palermo, B. A. Block, M. R. Reshotko, and P. L. D. Chang, "Optical I/O technology for Tera-scale computing," *IEEE J. Solid-State Circuits*, Vol. 45, 235–248, 2010.

115. Byun, G. S., Y. Kim, J. Kim, S. W. Tam, and M. C. F. Chang, "An energy-efficient and high-speed mobile memory I/O interface using simultaneous bi-directional dual (Base plus RF)-band signaling," *IEEE J. Solid-State Circuits*, Vol. 47, 117–130, 2012.

116. Kim, B., Y. Liu, T. O. Dickson, J. F. Bulzacchelli, and D. J. Friedman, "A 10-Gb/s compact low-power serial I/O with DFE-IIR equalization in 65-nm CMOS," *IEEE J. Solid-State Circuits*, Vol. 44, 3526–3538, 2009.

117. Joy, S. R., M. Erementchouk, H. Yu, and P. Mazumder, "Spoof plasmon interconnects-communications beyond RC limit," *IEEE Trans. Commun.*, Vol. 67, 599–610, 2019.

118. Guo, Y. J., K. D. Xu, X. J. Deng, X. Cheng, and Q. Chen, "Millimeter-wave on-chip bandpass filter based on spoof surface plasmon polaritons," *IEEE Electron Device Lett.*, Vol. 41, 1165–1168, 2020.

119. Xu, K. D., Y. J. Guo, Q. Yang, Y. L. Zhang, X. J. Deng, A. X. Zhang, and Q. Chen, "On-chip GaAs-based spoof surface plasmon polaritons at millimeter-wave regime," *IEEE Photonic Tech. L.*, Vol. 33, 255–258, 2021.

120. Lai, R. B., J. J. Kuo, and H. Wang, "A 60–110 GHz transmission-line integrated SPDT switch in 90 nm CMOS technology," *IEEE Microwave and Wireless Components Letters*, Vol. 20, 85–87, 2010.

121. Zhang, B., Y. Z. Xiong, L. Wang, and S. M. Hu, "A switch-based ASK modulator for 10 Gbps 135 GHz communication by 0.13 μm MOSFET," *IEEE Microwave and Wireless Components Letters*, Vol. 22, 415–417, 2012.

122. Meng, X. Y., B. Y. Chi, and Z. H. Wang, "A 152-GHz OOK transmitter with 3-dBm output power in 65-nm CMOS," *IEEE Microwave and Wireless Components Letters*, Vol. 27, 748–750, 2017.

123. Liang, Y., C. C. Boon, C. Y. Li, X. L. Tang, H. J. Ng, D. Kissinger, Y. Wang, Q. F. Zhang, and H. Yu, "Design and analysis of D-band on-chip modulator and signal source based on split-ring resonator," *IEEE Transactions on Very Large Scale Integration (Vlsi) Systems*, Vol. 27, 1513–1526, 2019.

124. He, P. H., H. C. Zhang, X. X. Gao, L. Y. Niu, W. X. Tang, J. Y. Lu, L. P. Zhang, and T. J. Cui, "A novel spoof surface plasmon polariton structure to reach ultra-strong field confinements," *Opto-Electronic Advances*, Vol. 2, 2019.

125. Zhang, H. C., T. J. Cui, Y. Luo, J. J. Zhang, J. Xu, P. H. He, and L. P. Zhang, "Active digital spoof plasmonics," *National Science Review*, Vol. 7, 261–269, 2020.

126. Zhang, H. C., L. P. Zhang, P. H. He, J. Xu, C. Qian, F. J. Garcia-Vidal, and T. J. Cui, "A plasmonic route for the integrated wireless communication of subdiffraction-limited signals," *Light-Sci. Appl.*, Vol. 9, 2020.